AFFDL-TR-67-195

INFLUENCE OF FREE-STREAM TURBULENCE ON HYPERSONIC STAGNATION ZONE HEATING

DR. THOMAS M. WEEKS

TECHNICAL REPORT AFFDL-TR-67-195

MAY 1968

AIR FORCE FLIGHT DYNAMICS LABORATORY
AIR FORCE SYSTEMS COMMAND
WRIGHT-PATTERSON AIR FORCE BASE, OHIO

NOTICE

When Government drawings, specifications, or other data are used for any purpose other than in connection with a definitely related Government procurement operation, the United States Government thereby incurs no responsibility nor any obligation whatsoever; and the fact that the Government may have formulated, furnished, or in any way supplied the said drawings, specifications, or other data, is not to be regarded by implication or otherwise as in any manner licensing the holder or any other person or corporation, or conveying any rights or permission to manufacture, use, or sell any patented invention that may in any way be related thereto.

This document has been approved for public release and sale; its distribution is unlimited.

Copies of this report should not be returned unless return is required by security considerations, contractual obligations, or notice on a specific document.

300 - June 1968 - CO155 - 38-825

INFLUENCE OF FREE-STREAM TURBULENCE ON HYPERSONIC STAGNATION ZONE HEATING

Thomas M. Weeks

Air Force Flight Dynamics Laboratory
Wright-Patterson Air Force Base, Ohio

May 1968

AFFDL-TR-67-195

INFLUENCE OF FREE-STREAM TURBULENCE ON HYPERSONIC STAGNATION ZONE HEATING

DR. THOMAS M. WEEKS

FOREWORD

This report was prepared by Lt T. M. Weeks of the Electrogasdynamics Branch, Air Force Flight Dynamics Laboratory, Wright-Patterson Air Force Base, Ohio. The work was conducted under Project No. 1426, "Experimental Simulation for Flight Mechanics," Task No. 142604, "Theory of Dynamic Simulation of Flight Environment (Dynamic Flight Simulation)."

The period of work covered by this report was from January 1966 to June 1967. This report was submitted by the author in November 1967 for publication.

This technical report has been reviewed and is approved.

Philip P. Antonatos

PHILIP P. ANTONATOS
Chief, Flight Mechanics Division
Air Force Flight Dynamics Laboratory

ABSTRACT

The much ignored problem of turbulence in hypersonic ground test facilities is discussed with particular emphasis on arc-heated facilities. Sources of free-stream turbulence and their effects on model aerodynamics are identified. An analytical treatment of stagnation zone heating accounting for free-stream vorticity amplification and viscous dissipation is presented. Results are discussed in relation to three experiments: one involving time resolved measurements in an arc-heated wind tunnel, another involves stagnation point heat transfer measurements in the turbulent boundary layer of a hypersonic shock tunnel, and the third deals with similar measurements in a turbulent subsonic nitrogen plasma jet. In both of the latter experiments, stagnation point heating rates exceeding two to three times the calculated laminar expectation are reported. These results are corroborated by the present analysis.

TABLE OF CONTENTS

ILLUSTRATIONS

SYMBOLS

A	Amplitude parameter
a	Scale factor in Hiemenz flow
$\vec{c}^*$	Fluid velocity vector
$\vec{c}$	Nondimensional fluid velocity vector
c_p	Specific heat at constant pressure
E	Dimensionless Eckert number (Equation 3)
k	Dimensionless wave number
N^*	Source term in energy equation (Equations 40, 41)
Pr	Prandtl number
q	Heat transfer rate
q_b	Heat transfer rate for A=E=O
R	Turbulence intensity ratio
T^*	Fluid temperature
T	Nondimensional fluid temperature
U, V, W	Nondimensional ξ, η, ζ components of fluid velocity, respectively
u, v, w	Disturbance velocity components
x_i	Coordinate axes (i = 1, 2, 3)
γ	Specific heat ratio
ξ, η, ζ	Nondimensional coordinate system
θ	Disturbance temperature
$\tilde{\Theta}$	Spectral interaction function (Equation 31)
λ	Wavelength
ν	Kinematic viscosity
ϕ	Velocity function (=-Vo)
Φ	Dissipation function (Equation 9)

SYMBOLS (CONT)

$\tilde{\Psi}$	Spectral interaction function (Equation 25)
Ω	x component of vorticity
ω	Disturbance vorticity

Subscripts

∞	Free stream
w	Wall
0	Mean value or zeroth harmonic
ξ, η, ζ	Differentiation
1, 2	Harmonic
(1), (2), (3)	Approximation

Primes denote differentiation with respect to η; a tilde over a symbol designates a spectral interaction function.

SECTION I

INTRODUCTION

The severe reentry environment, both present and future, places a heavy demand on ground test facilities to provide realistic simulation. A problem common to most hypersonic facilities which, until now, has been virtually ignored concerns the presence of free-stream turbulence. Broadly defined, hypersonic wind tunnel turbulence includes all unsteady flow behavior eventually experienced by the test article. Included therefore are gross property variations in the test affluent. To a first approximation, frozen disturbance patterns convected by the mean flow make up a significant portion of hypersonic turbulence. Inherent in the nature of hypersonic turbulence defined in this way is the lar change in scale of a given disturbance in passing from the hypersonic free stream to the model flow field. Thus free-stream disturbance wavelengths of the order of the tunnel size may become of classical size near a stagnation point.

There is growing evidence that such hypersonic turbulence significantly increases both stagnation region heating and ablation rates as well as reduces the transition Reynolds number when comparing these effects to laminar free-stream results.

This report discusses the general aspects of the overall problem. The turbulence is characterized and an analysis of stagnation line heat transfer based on earlier work of Sutera (Reference 1) is presented. The effects of both vorticity amplification and viscous dissipation are included. An incompressible flow of a perfect gas is assumed. Some experimental results are discussed which support the theory and provide specific evidence of the importance of the problem.

SECTION II

THE HYPERSONIC TURBULENCE PROBLEM

1. STATEMENT

A definition of hypersonic wind tunnel turbulence is given in Section I. Any spatiotemporal variation of any flow property about its mean value is a component of hypersonic turbulence. In a typical ground test facility, there exist certain cause and effect aspects which may be treated separately. The origin of the turbulence in a typical hypersonic facility (excluding the hypervelocity range facility) is clearly related to the particular driver. Figure 1 shows an arc-heated wind tunnel capable of providing hypersonic aerodynamic simulation or low Mach number simulation of high shear, high heat transfer. Several mechanisms which may render the flow turbulent are identified.

Fluctuations in arc heater supply voltage, current, and pressure are obvious sources of turbulence. If the arc is vortex stabilized, the rotational frequency is important. The heater itself may be, for a certain set of operating conditions, a source of natural longitudinal, radial, and circumferential acoustic resonance. The plasma turbulence in the cylindrical cavity consists conceivably of both solenoidal and irrotational modes as described by Kovasznay (Reference 2). The task of identifying various sources of unsteady flow behavior within the heater appears formidable owing to strong coupling effects.

As the flow is accelerated toward the throat, additional coupling of turbulence modes takes place due to large axial and radial property gradients. The fundamental character of the turbulence changes as the flow becomes supersonic. The various separate turbulence modes examined by Kovasznay (Reference 3) and Chu and Kovasznay (Reference 4) are the acoustic, vorticity, and entropy modes. In addition, there is a chemical mode which in arc-heated devices would include some contamination. Although nonlinear mode coupling still occurs near the throat and within the boundary layer, one expects that for small enough disturbance amplitudes the various modes are uncoupled in the free stream (Reference 3). If the nozzle boundary layer becomes turbulent, it is capable of producing additional free-stream turbulence in the form of acoustic radiation, which may be enhanced by probable vibration of water-cooled nozzle walls.

The origin and basic nature of the turbulence which ultimately appears in the test effluent have been characterized above. Any one of the described property variations in the heater can, by the mechanism of nonlinear mode coupling near the throat, give rise to all four turbulence modes in the test gas. For this reason, all hypersonic facilities operating in the range where chemical kinetics are important and having any kind of disturbance present in the driver are potentially capable of containing all forms of turbulence in the test core. This first aspect of the turbulence problem has been well documented for supersonic facilities (see Morkovin, Reference 5).

The second major aspect of the problem is concerned with the effects of the various free-stream turbulence modes on simulation. The three separate effects identified are (1) observed increased stagnation region heat transfer and skin friction (References 6 through 12), (2) incorrect mechanical ablation (Reference 13), and (3) early boundary layer transition (Reference 14). The ways in which the presence of free-stream turbulence brings about these effects are complex. Basically, each of the turbulence modes (acoustic, vorticity, entropy, chemical) is capable, upon shock interaction, of generating all four modes behind the shock (e.g., References 3 and 14 through 19). As an example, fluctuations in free-stream atomic oxygen concentration may yield fluctuations in velocity behind the bow shock wave. Behind the bow shock we may again, for high enough stagnation point Reynolds numbers, identify a flow region

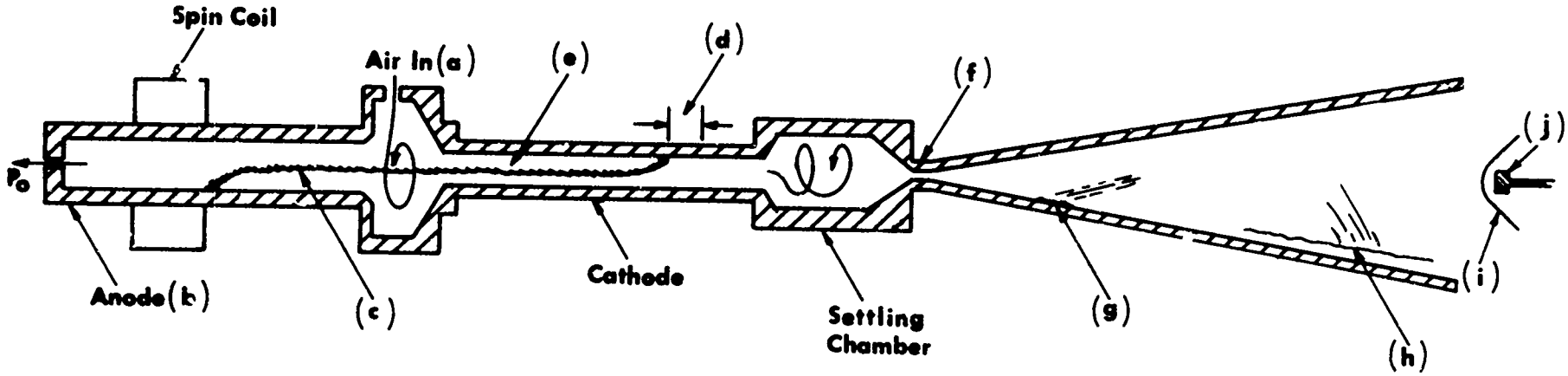

Sources of turbulence are a through i; j is principal effects.			
a	Mechanical Pumping	f	Turbulence Mode Coupling
b	Rectified D.C. 1 - 4 megawatts (300 Hz)	g	Surface Roughness
c	Arc Intermittency (200 kHz)	h	Turbulent Boundary Layer, Acoustic Radiation
d	Arc Foot Travel	i	Shock-Turbulence Interaction
e	Acoustic Modes (5 kHz)	j	Modified $\dot{q}$, $\dot{m}$, $Re_{critical}$

Figure 1. Schematic of Vortex Stabilized Arc-Heated Wind Tunnel

ahead of the boundary layer wherein the four modes are uncoupled. Convection of vorticity enthalpy and chemical modes and propagation of acoustic waves through the stagnation point boundary layer will alter the surface heat transfer rate and skin friction calculated by assuming laminar flow and laminar transport properties (including viscosity, conductivity, and species diffusion coefficients). The role of wall catalycity must be reaxamined, and surface catalytic efficiency will be seen to depend on boundary layer turbulence levels. Turbulent flow in the boundary layer will also quite naturally result in modified ablation patterns. Early transition to a turbulent boundary layer on the model bears an obvious connection to the free-stream turbulence level found in conventional supersonic wind tunnels.

It is not intended to suggest that each of the three effects exists separately because all three might be encountered in a typical hypersonic wind tunnel. The major point is, however, that for both cited applications of the arc-heated facility, i.e., hypersonic aerodynamic and high shear, high heat transfer simulation, the problem of free-stream turbulence must not be overlooked.

2. APPROACH

The first of two possible independent approaches to the problem of hypersonic wind tunnel turbulence is a direct attack aimed at eliminating, suppressing, or at least altering the character of the turbulence sources. The usual turbulence suppression devices, well understood in supersonic wind tunnels, cannot be installed in hyperthermal facilities without serious loss of total enthalpy. Of course, a high degree of rectification of the power supply and "compressor off" operation are indicated. Careful tuning of the heater may reduce acoustic resonance effects for a particular operating point. Fluctuations in arc length and attachment mode, a major contributor to effluent turbulence especially at high driver pressures, are still without apparent solution.

Another important suppression technique might be aimed at reducing property gradients in the throat region. The present day cone cyclinder-cone throat geometry would probably require modification. A suggestion based on experience with low power level choked flows indicates that uncooled graphite throats yield much quieter flows than highly cooled copper throats (Reference 20). It would appear that the greatly reduced radial temperature gradient in the graphite throat case reduced noise generation by the coupling mechanism previously described in this Section.

In order to bring about a reduction of arc-heated wind tunnel turbulence, it will be necessary to initially characterize the various modes of turbulence which are present. This may, in part, be accomplished via a number of flow diagnostic techniques currently available, although by no means well understood in the hyperthermal range. Thus one is led to consider the various flow visualization techniques including laser doppler schlieren and crossed optical beams (Reference 21), as well as inserted probe devices such as hot wire and cooled sensors (References 22 and 23), and acoustic and heat flux probes (see Section IV). A promising technique employing an electron beam with fiber optics has been used successfully (Reference 24).

The second approach, which can be carried out in large part independently of the first, involves the analysis of the effects of arbitrary forms of turbulence, characterized for example by amplitude, frequency, and correlation on model aerodynamics. Major emphasis should be given to whatever modes of turbulence are actually present in an arc-heated facility. At the present time, it would appear safe to assume, based on previous arguments, that all modes, albeit uncoupled in the free stream, are present. The presence of these free-stream turbulence modes results in modified stagnation zone flow which may be subdivided into two categories: (1) shock-turbulence interaction where the newly created or modified turbulence modes behind the bow shock must be identified and (2) the model boundary layer flow field having initially uncoupled turbulence modes at its outer edge. The order of attack is not

important, and each major component may be subdivided into various mode coupling problems, such as shock-vorticity (References 5 through 8); shock-chemical mode coupling; boundary layer-vorticity; boundary layer-acoustic mode coupling.

Recently, Sutera (References 1 and 25) analyzed the effects of free-stream vorticity amplification through a stagnation line boundary layer on skin friction and heat transfer. He found that both the skin friction and heat transfer increased (by different amounts) due to the presence of a specifically oriented upstream steady vorticity field convected through the boundary layer. The analysis was carried out assuming incompressible flow of a perfect gas. Provision was made to include the generation of higher harmonic spectral interaction functions including temperature-velocity coupling terms. Effects of viscous dissipation were not considered and the actual numerical solution was accomplished using truncated forms of the higher order approximations because of the limited analog computer capacity.

The effects of species diffusion should be included although, as stated previously in this Section, this analysis should be based on turbulent diffusion coefficients as yet not well known. It would appear then that a logical extension to Sutera's problem is to assess the effects of viscous dissipation and include all higher harmonic terms in the highest practical approximation. This represents, approximately, the flow field behind a hypersonic bow shock. One may regard the presence of the spatially distributed vorticity field as a direct result of shock-turbulence interaction.

SECTION III

TWO-DIMENSIONAL STAGNATION POINT HEAT TRANSFER WITH VORTICITY AMPLIFICATION AND VISCOUS DISSIPATION

1. MATHEMATICAL STATEMENT OF PROBLEM

The need to include effects of viscous dissipation arises from the result, obtained by Sutera et al (Reference 25), that a neutral scale vorticity exists. For turbulence wave lengths above this scale the mechanism of vorticity amplification is found. For wavelengths below this scale there is vorticity attenuation. Sutera attributes this to viscous dissipation but does not formally provide for this effect in the energy equation.

In this report, the basic approach to the problem initially parallels that of Sutera, i.e., the same basic form of the upstream vorticity with wavelength again equal to 1.5 times the neutral is chosen for purposes of comparison. Figure 2 shows the basic flow model. The added vorticity is in the only direction capable of amplification. The modified analysis begins with Sutera's form of the energy equation but with the viscous dissipation term included.

$$(\vec{c}^{\,*} \cdot \nabla)\, T^* = \frac{\nu}{Pr} \nabla^2 T^* + \sum_{i=1}^{3} \sum_{k=1}^{3} \frac{\nu}{2c_p} \left(\frac{\partial c_i^*}{\partial x_k} + \frac{\partial c_k^*}{\partial x_i} \right) \qquad (1)$$

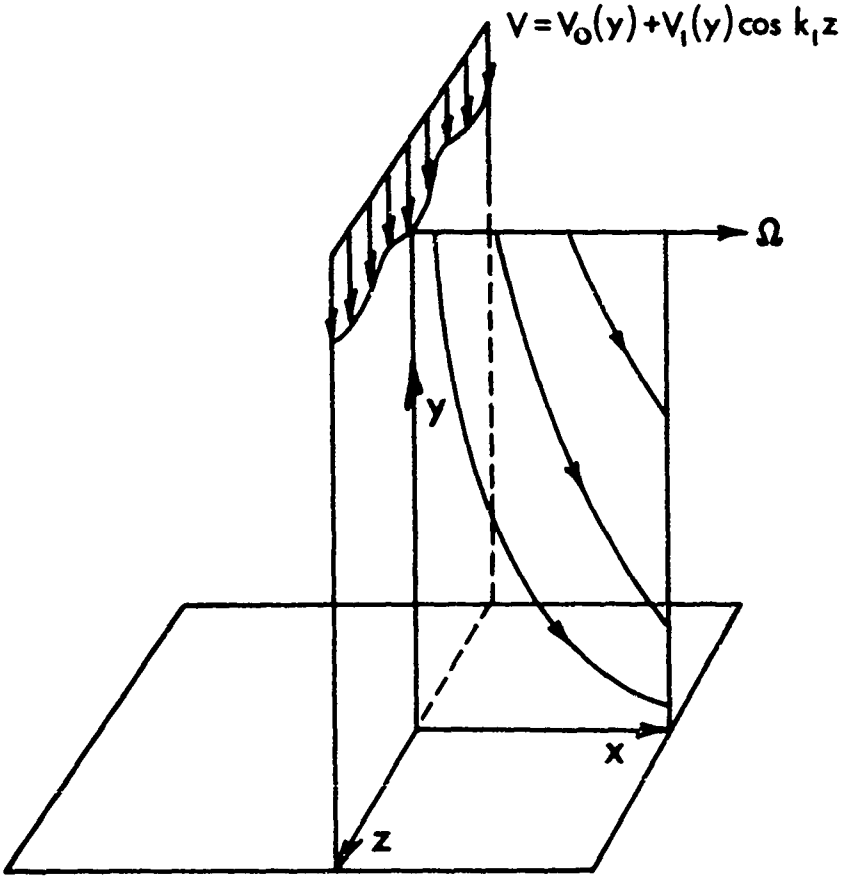

Figure 2. Hiemenz Flow Field With Added Vorticity

Specializing to the Hiemenz flow configuration which employs nondimensional flow quantities and the same scale factor one has:

$$(\vec{c}\cdot\nabla)T = \frac{1}{Pr}\nabla^2 T + \frac{a\nu}{c_p(T_\infty - T_w)}\cdot\Phi \tag{2}$$

The quantity $\sqrt{a\nu}$ has been used to nondimensionalize the velocity and one recognizes the dimensionless Eckert number:

$$E = \frac{a\nu}{c_p(T_\infty - T_w)} \tag{3}$$

Note also that the quantity $\sqrt{\nu/a}$ has the dimensions of length. The complete system of governing differential equations expanded into the ξ, η, ζ nondimensional coordinate system becomes (Reference 1):

$$V\Omega_\eta + W\Omega_\zeta - \Omega U = \Omega_{\eta\eta} + \Omega_{\zeta\zeta} \tag{4}$$

$$UU_\zeta + VU_{\zeta\eta} + WU_{\zeta\zeta} - U_\zeta V_\eta + U_\eta V_\zeta = (U_{\eta\eta} + U_{\zeta\zeta})_\zeta \tag{5}$$

$$UU_\eta + VU_{\eta\eta} + WU_{\eta\zeta} + U_\zeta W_\eta - U_\eta W_\zeta = (U_{\eta\eta} + U_{\zeta\zeta})_\eta \tag{6}$$

$$U + V_\eta + W_\zeta = 0 \tag{7}$$

$$VT_\eta + WT_\zeta = \frac{1}{Pr}(T_{\eta\eta} + T_{\zeta\zeta}) + E\cdot\Phi \tag{8}$$

where

$$\Phi = 2(U^2 + V_\eta^2 + W_\zeta^2 + V_\zeta W_\eta) + W_\eta^2 + V_\zeta^2 \tag{9}$$

It has been assumed in Equations 4 through 9 that terms involving ξ^2 in the dissipation function could be neglected. This, of course, restricts the solution to a region close to the stagnation line. Next, it is assumed that the three-dimensional nature of the turbulent flow field may be characterized by the following Fourier structure which permits solutions periodic in ζ.

$$\begin{aligned} U &= U_o(\eta) + A\sum_{n=1}^{\infty} u_n(\eta)\cos k_n\zeta \\ V &= V_o(\eta) + A\sum_{n=1}^{\infty} v_n(\eta)\cos k_n\zeta \\ W &= \sum_{n=1}^{\infty}\frac{1}{k_n} W_n(\eta)\sin k_n\zeta \\ T &= T_o(\eta) + A\sum_{n=1}^{\infty}\theta_n(\eta)\cos k_n\zeta \end{aligned} \tag{10}$$

The harmonic coefficients u_n, v_n, θ_n are not necessarily small with respect to their mean flow counterparts U_o, V_o, T_o, respectively. Substitution of Equations 10 into Equations 4 through 8 leads ultimately to a set of two plus a quintuple infinity of ordinary nonlinear differential equations with as many unknowns. These equations express both mean and "fluctuating" quantities as functions of distance from the wall. The detailed set of equations without viscous dissipation appears as Equations 18 through 27 of Reference 1. The energy equation governing the mean temperature variation modified to include dissipation becomes:

$$T_o'' + Pr\,\phi\,T_o' + 4E\,Pr\,\phi'^2 = \frac{A^2}{2}\,Pr\sum_{i=1}^{\infty}\left[u_i\,\theta_i + (v_i\,\theta_i)'\right]$$
$$-A^2\,Pr\,E\sum_{i=1}^{\infty}\left[2(u_i^2 + w_i^2 + v_i'^2) - 2v_i\,w_i' + (v_i\,k_i)^2 + (w_i'/k_i)^2\right] \tag{11}$$

The fluctuating temperature field is governed by the following expression:

$$\theta_n'' + Pr\,\phi\,\theta_n' - \theta_n\,k_n^2 - Pr\,T_o'\,v_n + 4E\,Pr\,\phi'(u_n - v_n') = \frac{A}{2}\,Pr\,(I_{1,n} - I_{2,n})$$
$$-AE\,Pr\,(I_{3,n} + I_{4,n} + I_{5,n} - I_{6,n} + I_{7,n} + I_{8,n}) \tag{12}$$

The Spectral interaction functions $I_{(\alpha,n)}$ are tabulated in the Appendix. It may be seen that even without free-stream turbulence (A=o) there is a viscous dissipation effect owing to the finite value of $U_o = -V_o' = \phi'$. Solutions of the entire system of equations have been obtained by means of an analog computer and a digital computer simulation of the analog computer program.

2. ANALOG COMPUTER SOLUTION

It is necessary to choose a wave number, k_1, for the first harmonic component of the initial velocity and temperature field. Sutera has considered a simple sinusoidal variation of the normal velocity which corresponded to a single value of k_1 at the outer edge of the boundary layer. One can, in principle, include additional wave numbers to more closely represent a hypothetical turbulent velocity distribution. Such a modification would not alter the fundamental heat transfer mechanisms under examination and would unnecessarily complicate the analysis. The appearance of higher harmonics within the boundary layer is included in the analysis and it is seen that only the second harmonic terms must be retrained.

The most appropriate wave number to choose is one which exceeds the neutral scale value thus ensuring that both the vorticity amplification and viscous dissipation mechanisms will be effective. It is necessary, therefore, that $k_1 < 1$ which is the same as $\lambda_1 > \lambda_o$ where λ_o is the neutral wavelength. To facilitate direct comparison with Sutera's result, a value of $k_1 = 2/3$ was chosen. A range of the turbulence amplitude parameter A was considered for several values of the stagnation zone Eckert number. The latter values were chosen about the usual narrow range encountered in hypersonic facilities.

The iterative solution began by assuming that, to first approximation, the spectral interaction functions contribute nothing to the velocity and vorticity components. The homogeneous forms of the governing equations were solved simultaneously and provided a first approximation to the

first and second harmonic components (n=1,2) of velocity and vorticity interaction terms. These components were then substituted into the governing equations to yield a second approximation to the velocity and vorticity field. This procedure generates a second approximation to both the first and second harmonic spectral interaction functions. These results were applied to the energy equations (both mean and harmonic forms) to obtain first approximations to the spectral temperature-velocity interaction functions which finally yield values of the mean temperature field.

The actual calculation scheme as it was programmed for the analog computer and subsequently written in MIMIC (digital simulation) is presented below. The set of homogeneous differential equations governing the first approximation to the first harmonic velocity and vorticity components are listed first

$$\phi'''_{(1)} + \phi_{(1)}\phi''_{(1)} - \phi'^{2}_{(1)} + 1 = 0 \tag{13}$$

(See Schlichting, Reference 26)

$$-v''_{1(1)} + \frac{4}{9} v_{1(1)} - \frac{4}{3} \omega_{1(1)} - u'_{1(1)} = 0 \tag{14}$$

$$u''_{1(1)} + \phi_{(1)} u'_{1(1)} - u_{1(1)} \left(2\phi'_{(1)} + \frac{4}{9}\right) - \phi''_{(1)} v_{1(1)} \tag{15}$$

$$w_{1(1)} = -v'_{1(1)} - u_{1(1)} \tag{16}$$

The corresponding boundary conditions to be imposed are:

$$\phi_{(1)}(0) = \phi'_{(1)}(0) = 0 \; ; \; \phi''_{(1)}(0) = 1.237$$

$$v_{1(1)}(0) = v'_{1(1)}(0) = 0$$

$$u_{1(1)}(0) = 0$$

$$\phi'_{(1)} \longrightarrow \text{as } \eta \longrightarrow \infty$$

$$v'_{1(1)}, v''_{1(1)}, u_{1(1)} \longrightarrow 0 \text{ as } \eta \longrightarrow \infty$$

A boundary search routine was employed in the MIMIC program and the solution to Equations 13 through 15 was obtained. Spectral velocity interaction functions were defined:

$$\tilde{\Omega}_{2(1)} = \omega_{1(1)} v_{1(1)} + \omega'_{1(1)} v_{1(1)} + 2 w_{1(1)} \omega_{1(1)}$$

and

$$\tilde{U}_{2(1)} = 2\left(u^{2}_{1(1)} + w_{1(1)} u_{1(1)}\right) + \left(v_{1(1)} u'_{1(1)} + v'_{1(1)} u_{1(1)}\right)$$

Then the governing equations for a first approximation to the second harmonic ($k_2 = 4/3$) velocity (and vorticity) components become:

$$-v''_{2(1)} + \frac{16}{9} v_{2(1)} - \frac{8}{3} \omega_{2(1)} - u'_{2(1)} = 0 \tag{17}$$

$$\omega''_{2(1)} + \phi_{(1)} \omega'_{2(1)} + \phi_{(1)} \omega_{2(1)} - \frac{16}{9} \omega_{2(1)} = \frac{A}{2} \tilde{\Omega}_{2(1)} \tag{18}$$

$$u''_{2(1)} + \phi_{(1)} u_{2(1)} - u_{2(1)} \left(2\phi'_{(1)} + \frac{16}{9}\right) - \phi''_{(1)} v_{2(1)} = \frac{A}{2} \tilde{U}_{2(1)} \tag{19}$$

$$w_{2(1)} = - v'_{2(1)} - u_{2(1)} \tag{20}$$

The boundary conditions are:

$$v_{2(1)}(0) = v'_{2(1)}(0) = u_{2(1)}(0) = 0$$

$$v'_{2(1)}, v''_{2(1)}, u_{2(1)} \to 0 \quad \text{as} \quad \eta \to \infty$$

Solutions of this set of equations were utilized to obtain the following interaction functions:

$$\tilde{\Omega}_{1(2)} = -\omega_{1(1)} v'_{2(1)} - \omega'_{1(1)} v_{2(1)} - w_{1(1)} \omega_{2(1)} + \omega_{2(1)} v'_{1(1)} + \omega'_{2(1)} v_{1(1)} - \frac{1}{2} w_{2(1)} \omega_{1(1)}$$

and

$$\tilde{U}_{1(2)} = 4u_{1(1)} u_{2(1)} + v_{1(1)} u'_{2(1)} + v'_{1(1)} u_{2(1)} - w_{1(1)} u_{2(1)}$$

$$+ v'_{2(1)} u_{1(1)} + v_{2(1)} u'_{1(1)} + \frac{1}{2} w_{2(1)} u_{1(1)}$$

The next step was to calculate the second approximation to the first harmonic velocity and vorticity field.

$$u'_{1(2)} - v''_{1(2)} + \frac{4}{9} v_{1(2)} - \frac{4}{3} \omega_{1(2)} = 0 \tag{21}$$

$$\omega''_{1(2)} + \phi_{(1)} \omega'_{1(2)} + \phi'_{(1)} \omega_{1(2)} - \frac{4}{9} \omega_{1(2)} = \frac{A}{2} \tilde{\Omega}_{1(2)} \tag{22}$$

$$u''_{1(2)} + \phi_{(1)} u'_{1(2)} - u_{1(2)} \left(2\phi'_{(1)} + \frac{4}{9}\right) - \phi''_{(1)} v_{1(2)} = \frac{A}{2} \tilde{U}_{1(2)} \tag{23}$$

$$w_{1(2)} = v'_{1(2)} - u_{1(2)} \tag{24}$$

The boundary conditions are:

$$v_{1(2)}(0) = v'_{1(2)}(0) = u_{1(2)}(0) = 0$$

$$v'_{1(2)}, v''_{1(2)}, u_{1(2)} \to 0 \text{ as } \eta \to \infty$$

The final velocity-vorticity interaction functions obtained were:

$$\tilde{\Omega}_{2(2)} = \omega_{1(2)} v'_{1(2)} + \omega'_{1(2)} v_{1(2)} + 2 w_{1(2)} \omega_{1(2)}$$

and

$$\tilde{U}_{2(2)} = 2 (u^2_{1(2)} + w_{1(2)} u_{1(2)}) + (v_{1(2)} u_{1(2)})'$$

A correction function for ϕ representing contributions of the spectral interaction function to the mean velocity field was also calculated.

$$\tilde{\Psi}_2 = u^2_{1(2)} + \frac{1}{2} (u_{1(2)} v'_{1(2)} + u'_{1(2)} v_{1(2)}) + u^2_{2(1)} + \frac{1}{2} (u_{2(1)} v'_{2(1)} + u'_{2(1)} v_{2(1)})$$

which yielded a second approximation for ϕ, i.e.,

$$\phi'''_{(2)} + \phi_{(2)} \phi''_{(2)} - \phi'^2_{(2)} + 1 = A^2 \tilde{\Psi}_{(2)} \tag{25}$$

The final system of equations solved for the velocity and temperature field corresponded to the second approximation, second harmonic components.

$$u'_{2(2)} - v''_{2(2)} + \frac{16}{9} v_{2(2)} - \frac{8}{3} \omega_{2(2)} = 0 \tag{26}$$

$$\omega''_{2(2)} + \phi'_{(2)} \omega_{2(2)} + \phi'_{(2)} \omega'_{2(2)} - \frac{16}{9} \omega_{2(2)} = \frac{A}{2} \tilde{\Omega}_{2(2)} \tag{27}$$

$$u''_{2(2)} + \phi'_{(2)} u'_{2(2)} - u_{2(2)} (2\phi'_{(2)} + \frac{16}{9}) - \phi''_{(2)} v_{2(2)} = \frac{A}{2} \tilde{U}_{2(2)} \tag{28}$$

$$w_{2(2)} = -v'_{2(2)} - u_{2(2)} \tag{29}$$

The boundary conditions are:

$$v_{2(2)}(0) = v'_{2(2)}(0) = u_{2(2)}(0) = 0$$

$$v'_{2(2)}, v''_{2(2)}, u_{2(2)} \longrightarrow 0 \quad \text{as} \quad \eta \longrightarrow \infty$$

A third approximation to ϕ was obtained, i.e.,

$$\phi'''_{(3)} + \phi_{(3)} \phi''_{(3)} - \phi'^2_{(3)} + 1 = A^2 \tilde{\Psi}_{(3)} \tag{30}$$

where

$$\tilde{\Psi}_{(3)} = u^2_{1(2)} + \frac{1}{2} (u_{1(2)} v'_{1(2)} + u'_{1(2)} v_{1(2)}) + u^2_{2(2)} + \frac{1}{2} (u_{2(2)} v'_{2(2)} + u_{2(2)} v_{2(2)})$$

The system of Equations 11 and 12 governing the mean and fluctuating temperature required several spectral velocity interaction functions defined as follows:

$$\tilde{\Theta}_{(1)} = 8\left[u_{1(2)}u_{2(2)} + v'_{1(2)}v_{2(2)} + w_{2(2)}w_{1(2)}\right] + \frac{16}{9}v_{1(2)}v_{2(2)} + \frac{9}{4}w'_{2(2)}w_{1(2)} - w'_{2(2)}v_{1(2)} - 4w_{1(2)}v_{2(2)} \tag{31}$$

$$\tilde{\Theta}_{(2)} = 4\left[u^2_{1(2)} + v'^2_{1(2)} + w^2_{1(2)}\right] - \frac{16}{9}v^2_{1(2)} - \frac{9}{16}w'^2_{1(2)} + 2w'_{1(2)}v_{1(2)} \tag{32}$$

$$\tilde{T}_{(2)} = 2\left(u^2_{1(2)} + w^2_{1(2)} + v'^2_{1(2)} + u^2_{2(2)} + w^2_{2(2)} + v'^2_{2(2)}\right) + \frac{1}{2}\left(\frac{2}{3}v_{1(2)} - \frac{3}{2}w'_{1(2)}\right)^2 + \frac{1}{2}\left(\frac{4}{3}v_{2(2)} - \frac{3}{4}w'_{2(2)}\right)^2 \tag{33}$$

The first approximation to the mean temperature field is obtained from Equation 11.

$$Pr\ T'_{0(1)}\phi_{(3)} + T''_{0(1)} + 4E\ Pr\ \phi'^2_{(3)} = 0 \tag{34}$$

with boundary conditions:

$$T_{0(1)}(0) = 0$$

$$T_{0(1)} \to 1\ ;\ T'_{0(1)},\ T''_{0(1)} \to 0 \text{ as } \eta \to \infty$$

The first approximation to the first harmonic component of the fluctuating temperature field is obtained from Equation 12 which becomes:

$$\theta''_{1(1)} + Pr\ \theta'_{1(1)}\phi_{(3)} - \frac{4}{9}\theta_{1(1)} = Pr\ T'_{0(1)}v_{1(2)} + 4E\ Pr\ \phi'_{(3)}\left[v'_{1(2)} - u_{1(2)}\right] + \frac{APr}{2}\left(I_{(1,1)} - I_{(2,1)}\right) - AE\ Pr\sum_{\alpha=3}^{8} I_{(\alpha,1)} \tag{35}$$

The spectral interaction functions $I_{(\alpha,1)}$ are listed in the Appendix. Appropriate boundary conditions take the form:

$$\theta_{1(1)}(0) = 0\ ;\ \theta_{1(1)} \to 0 \text{ as } \eta \to \infty$$

The first approximation to the second harmonic component of the fluctuating temperature field may be evaluated from:

$$\theta''_{2(1)} + Pr\ \theta'_{2(1)}\phi_{(3)} - \frac{16}{9}\theta_{2(1)} = Pr\ T'_{0(1)}v_{2(2)} + 4E\ Pr\ \phi'_{(3)}\left[v'_{2(2)} - u_{2(2)}\right] + \frac{APr}{2}\left[I_{(1,2)} - I_{(2,2)}\right] - AE\ Pr\sum_{\alpha=3}^{8} I_{(\alpha,2)} \tag{36}$$

with boundary conditions:

$$\theta_{2(1)}(0) = 0; \quad \theta_{2(1)} \longrightarrow 0 \quad \text{as} \quad \eta \longrightarrow \infty$$

We are now in a position to evaluate the second approximation to the mean temperature field.

$$T''_{o(2)} + Pr\ \phi_{(3)}\ T'_{o(2)} + 4E\ Pr\ \phi'^{2}_{(3)} = \frac{A^2 Pr}{2}\left[I_1 + E I_2\right] \tag{37}$$

where

$$I_1 = u_{1(2)}\theta_{1(1)} + (v_{1(2)}\theta_{1(1)})' + u_{2(2)}\theta_{2(1)} + (v_{2(2)}\theta_{2(1)})'$$

$$I_2 = 2\,(u^2_{1(2)} + v'^2_{1(2)} + w^2_{1(2)}) - 2\,v_{1(2)}w'_{1(2)} + \frac{4}{9}\,v^2_{1(2)} + \frac{9}{4}\,w'^2_{1(2)}$$

$$+ 2\,(u^2_{2(2)} + v'^2_{2(2)} + w^2_{2(2)}) - 2\,v_{2(2)}w'_{2(2)} + \frac{16}{9}\,v^2_{2(2)} + \frac{9}{16}\,w'^2_{1(2)}$$

Solution of Equation 37 provides necessary input to the calculation of the second approximation to the first harmonic component of the fluctuating temperature field which is obtained from the relation:

$$\theta''_{1(2)} + Pr\ \theta'_{1(2)}\ \phi_{(3)} - \frac{4}{9}\,\theta_{1(2)} = Pr\ T'_{o(2)}\,v_{1(2)} + 4E\ Pr\ \phi'_{(3)}\left[v'_{1(2)} - u_{1(2)}\right] + \frac{A\,Pr}{2}\left(I_{(1,1)} - I_{(2,1)}\right) - AE\ Pr \sum_{\alpha=3}^{8} I_{(\alpha,1)} \tag{38}$$

The second and final approximation to the second harmonic component of the fluctuating temperature field may be obtained from:

$$\theta''_{2(2)} + Pr\ \theta'_{2(2)}\ \phi_{(3)} - \frac{16}{9}\,\theta_{2(2)} = Pr\ T'_{o(2)}\,v_{2(2)} + 4E\ Pr\ (v'_{2(2)} - u_{2(2)}) + \frac{A\,Pr}{2}\left[I_{(1,2)} - I_{(2,2)}\right] - AE\ Pr \sum_{\alpha=3}^{8} I_{(\alpha,2)} \tag{39}$$

The results obtained above may be combined to provide a third and final approximation to the mean temperature field.

$$T''_{o(3)} + Pr\ \phi_{(3)}\,T'_{o(3)} + 4E\ Pr\ \phi'^{2}_{(3)} = \frac{A^2 Pr}{2}\left[I_1 + E I_2\right] \tag{40}$$

Where, consistent with the utilization of the best available approximation, we have:

$$I_1 = u_{1(2)}\theta_{1(2)} + (v_{1(2)}\theta_{1(2)})' + u_{2(2)}\theta_{2(2)} + (v_{2(2)}\theta_{2(2)})'$$

and I_2 remains unchanged.

3. RESULTS OF ANALYSIS

The important results of the analysis are, of course, the effects of vorticity amplification by vortex stretching and of viscous dissipation of vorticity on stagnation line heat transfer. It is worthwhile in this connection to examine the intensity amplification of the first and second harmonic components of v and u referred to the corresponding local mean velocity. Thus we may define the "turbulence intensity" ratios.

$$R_{1,1} = \left| u_{1(2)} \right| / U_0$$

$$= \left| u_{1(2)} \right| / \phi'_{(3)}$$

$$R_{1,2} = \left| v_{1(2)} \right| / V_0$$

$$= \left| v_{1(2)} \right| / \phi_{(3)}$$

$$R_{2,1} = \left| u_{2(2)} \right| / \phi'_{(3)}$$

$$R_{2,2} = \left| v_{2(2)} \right| / \phi_{(3)}$$

These ratios, plotted in Figure 3 as a function of y, depict the way in which the harmonic components of the disturbance velocity field are amplified over and above the corresponding local mean velocity as the flow approaches the wall. This behavior is in qualitative agreement with the results of Reference 27. Included is Sutera's (Reference 1) result for $r = \left| V_{1(1)} \right| / V_0$. One sees that Sutera predicts a relative intensity amplification which exceeds unity and also displays a maximum for $\eta > 0$. The present result predicts a peak intensity of 0.8 at $\eta = 0$. One may still conclude, however, that there is of the order of a hundredfold amplification of initial longitudinal velocity intensity. The first harmonic component of the lateral intensity attains a much smaller magnitude (a maximum of 4%). The corresponding second harmonic intensities are also of smaller magnitude than the longitudinal first harmonic. The longitudinal second harmonic intensity displays a double maximum owing to a sign change in $V_{2(2)}$.

The combined effects of vorticity amplification and viscous dissipation may be understood by examining the source term in Equation 40. Thus we may define:

$$N^* = \frac{A^2 Pr}{2} \left[I_1 + E I_2 \right] - 4 E Pr \phi'^2_{(3)} \qquad (41)$$

This reduces in form to Sutera's N_1 for A=1, E=0. Plots of N* vs η appear as Figure 4. In the case of laminar flow (A=0) we find that the source term is non-zero for E > 0. One may examine the variation of N* as a function of A alone only for the case that E=0. For E > 0 one cannot separate the two effects owing to the middle term in Equation 41.

Solutions of Equation 40 in the form of $T_{0_{(3)}}$, $T'_{0_{(3)}}$ are plotted vs η in Figure 5 for the same range of A and E as appears in Figure 4. The overall effect of increasing E is to increase the wall temperature gradient and reduce the thickness of the thermal boundary layer.

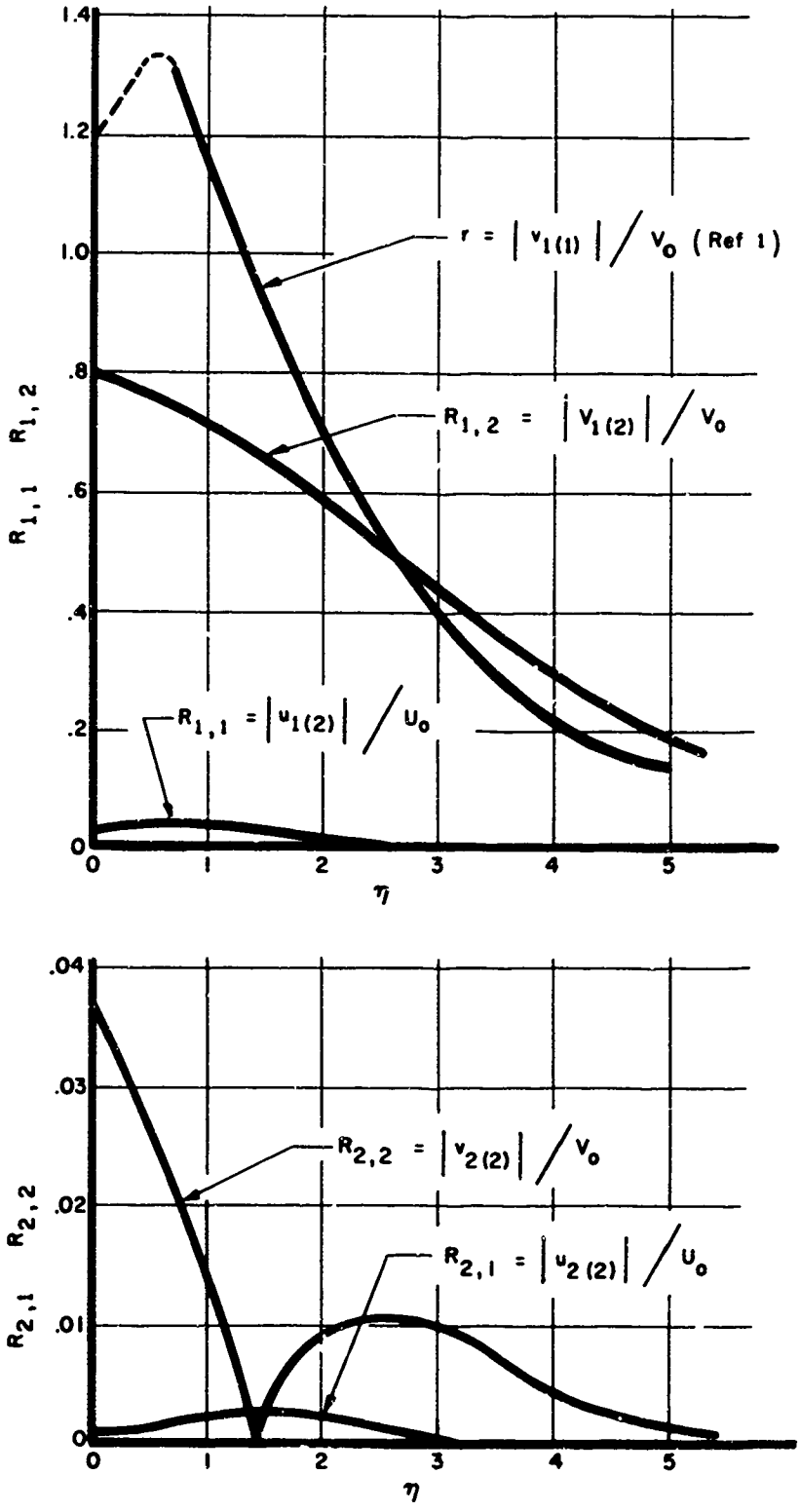

Figure 3. Relative Intensity Amplification of First and Second Harmonic Components of Longitudinal and Lateral Velocity Components

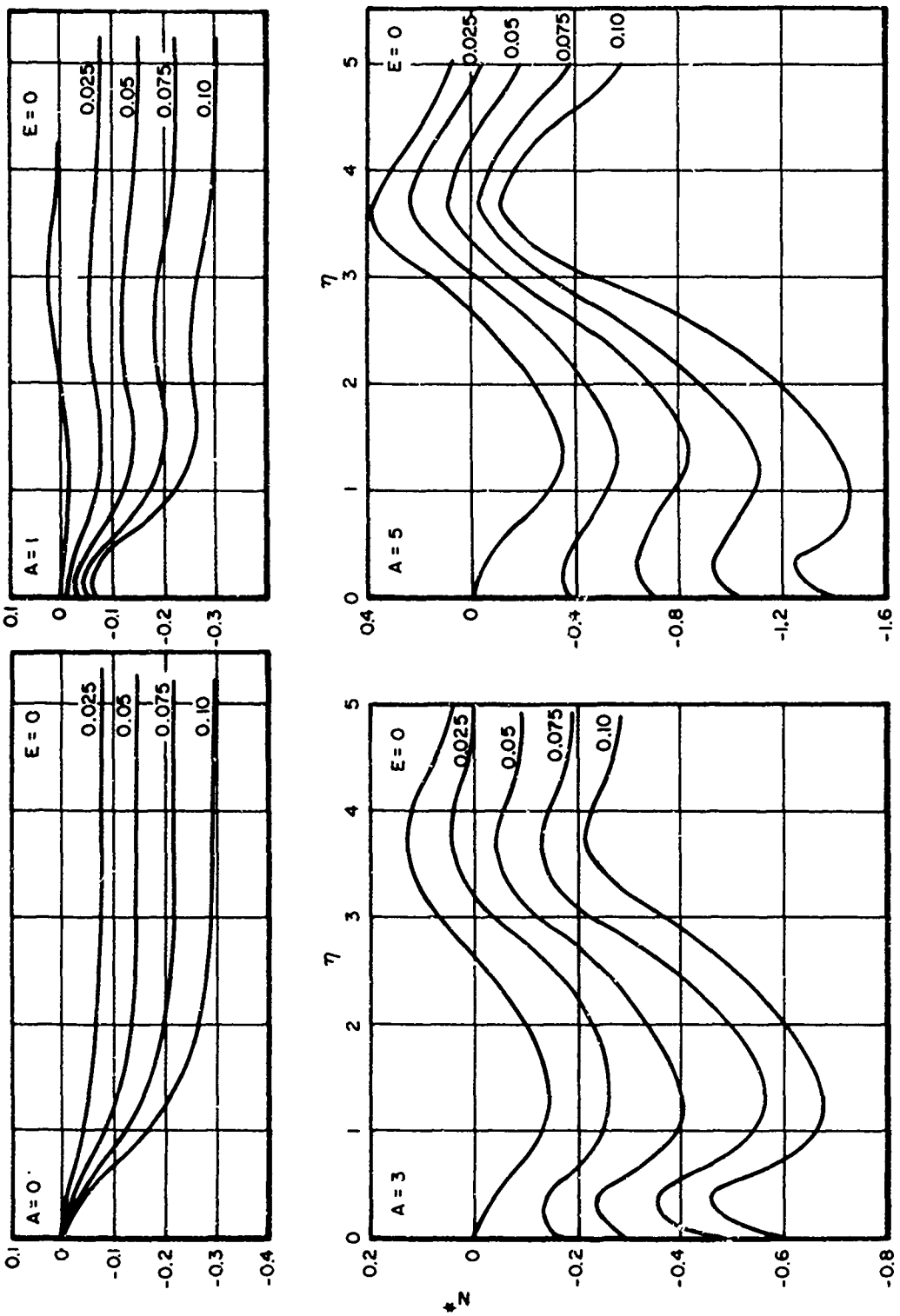

Figure 4. Source Term in Energy Equation (Equation 40) Includes Both Effects of Viscous Dissipation and Vorticity Amplification

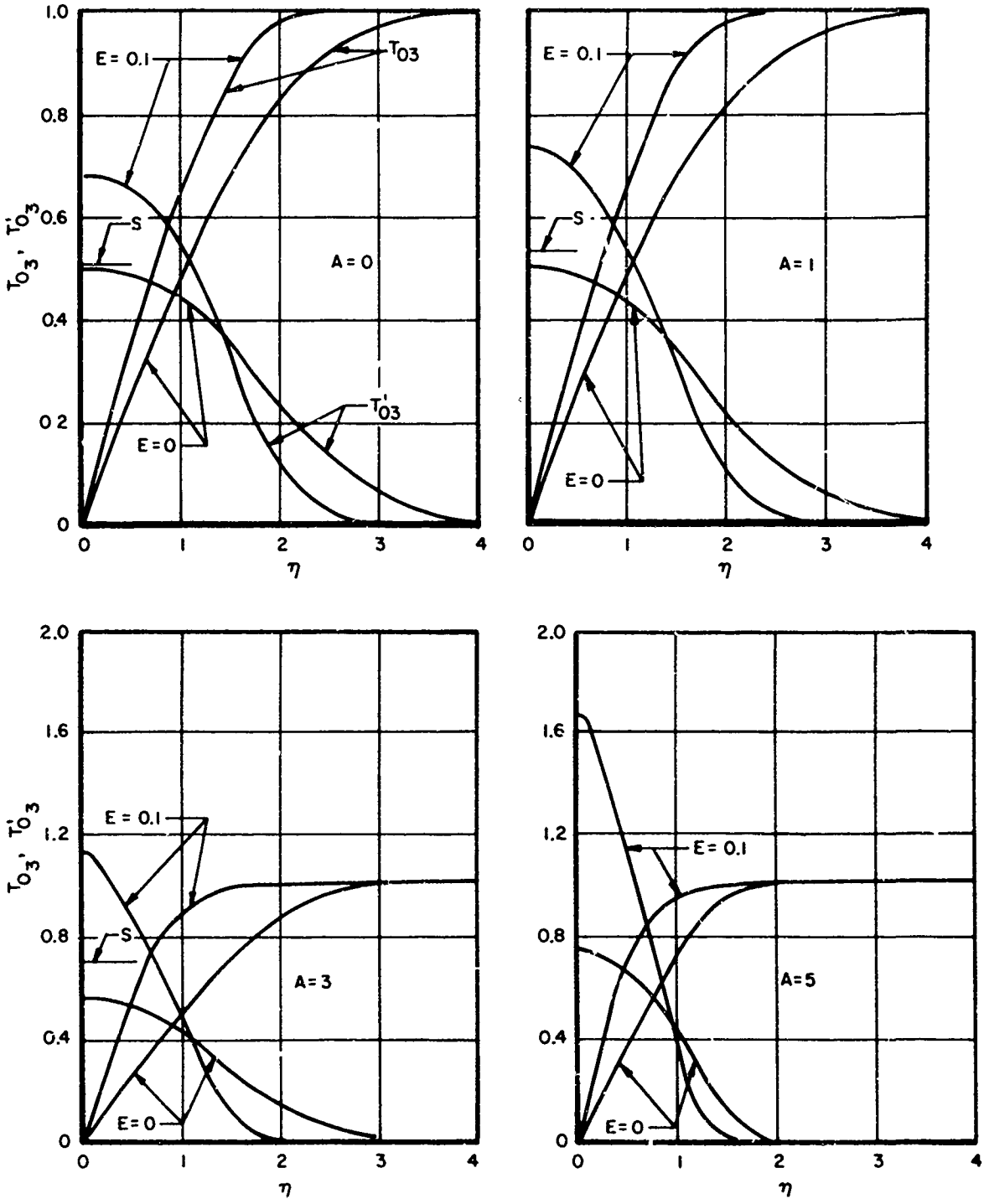

Figure 5. Mean Temperature and Temperature Gradient Illustrating Distortion Due To Viscous Dissipation and Vorticity Amplification

The level of $T_{o_{(3)}}$ labeled "S" is Sutera's value of $T_{o_{(2)}}$. This level which is to be compared with the E=O solution is somewhat higher in all cases, the difference increasing with the value of A.

We come finally to the most significant result, namely the wall heat transfer rate, q which is proportional to $T'_{o_{(3)}}(O)$. For a reference q_b we chose $T'_{o_{(3)}}(O)$ for A = E = O which has a value of 0.499. Dividing other wall values of $T'_{o_{(3)}}$ by this value, we can show in Figure 6 that the effects of both vorticity amplification and viscous dissipation are to significantly increase stagnation line heat transfer. As previously indicated in this Section, owing to the large gradient in V_o near the wall there is finite viscous dissipation even for laminar flow. One would expect, therefore, that even in free flight an underestimation of stagnation heat transfer at a leading edge will arise (the level depending on the magnitude of E) if viscous dissipation is not accounted for. One observes that the effect of increasing A (as noted by Sutera) or E is to increase the stagnation zone heat transfer. The effect of viscous dissipation is initially linear but is gradually reduced as the boundary layer becomes thinner. This is due to the fact that the source terms N* in Equation 40 (see Figure 4) while themselves extending well beyond the classical Hiemenz boundary layer have reduced influence on the thermal boundary layer which grows thinner with increasing E. This effect was observed by Sutera for increasing Prandtl number.

Included in Figure 6 are four calculated values for the Eckert number corresponding to the stagnation flow region of both an air arc-heated wind tunnel where $\gamma_f = 1.2$ and a perfect gas facility where $\gamma = 1.4$. In two cases (a, b) the hypersonic limiting value of $M_2 \approx 0.4$ was chosen. In the third case (c) a free-stream Mach number $M_1 = 2$, $\gamma_f = 1.2$ was selected. The final case represents a conventional supersonic wind tunnel condition with $\gamma = 1.4$, $M_1 = 3$. Transonic and subsonic wind tunnels would appear with still higher values of E. In all cases the Eckert number was obtained from the relation

$$E = (\gamma - 1)\, M_2^2 \tag{42}$$

The values obtained checked well with Eckert numbers calculated directly from the definition (Equation 3).

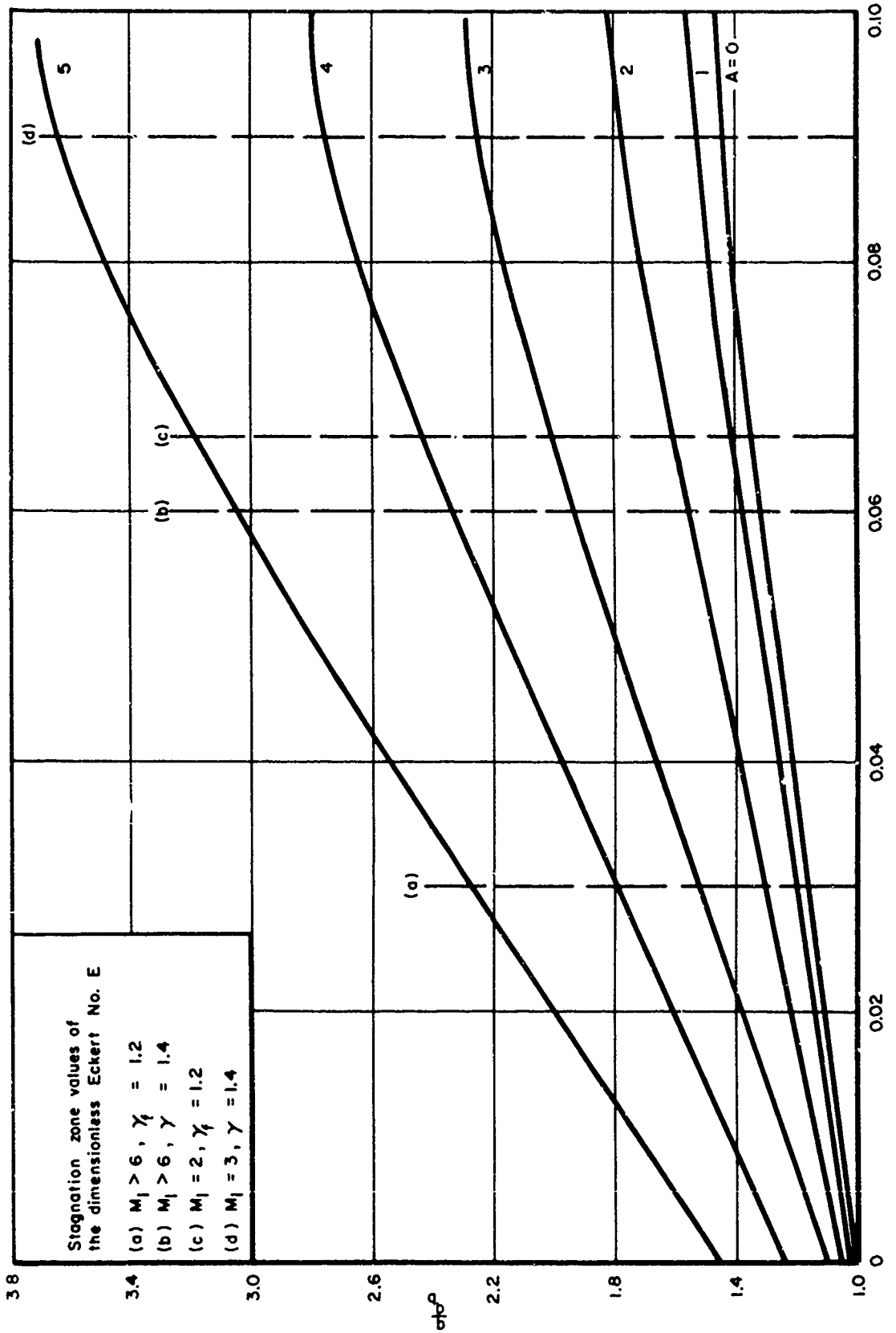

Figure 6. Heat Transfer Rate Referred To Value Corresponding to E=A=O

SECTION IV

EXPERIMENTAL RESULTS

1. SHOCK TUNNEL TURBULENT NOZZLE BOUNDARY LAYER

Some recent measurements by J. E. Wallace (Reference 28) of stagnation point heat transfer obtained with axisymmetric probes in a shock tunnel nozzle wall boundary layer provide a comparison with the theoretical predictions obtained in Section III It was found that "much higher heating rates occurred in the boundary layer than would be predicted based on measured pitot pressure profiles and an assumed Crocco energy relation for the total enthalpy variation." The reason was attributed to the free-stream turbulence described in References 1, 6, and 7.

In order to construct such a comparison it is necessary to relate the parameter A to the initial turbulence amplitude $|v|/V_o$ ahead of the probe boundary layer. Since the two are linearly related we need only to establish a single data point where both the excess heating over and above the laminar flow value as well as the free-stream longitudinal turbulence level are known. Of course one would expect that a meaningful comparison must necessarily be limited to two-dimensional configurations. Nevertheless, one may anticipate that the proper order of magnitude effects for axisymmetric shapes would be characterized. It is more than likely, however, that the constant of proportionality between A and $|v|/V_o$ is different for the two cases.

Short et al (Reference 9) reported measurements of both free-stream turbulence and corresponding heat transfer rates from a 0.5 inch diameter sphere in a low speed (16 fps) flow. They reported that an overall heat transfer increase of 20% accompanied a free-stream turbulence increase from 0.013 to 0.15. If we assume that at the lower reported turbulence level the heat transfer corresponds nearly to the laminar rate, we find from Figure 6 a value of A = 3.8 corresponding to E=O and $q/q_b = 1.2$. This provides a relation between A and $|v|/V_o$ for axisymmetric bodies in subsonic flow of the form:

$$A = \left(\frac{3.8}{0.15}\right)\left|v\right|/V \tag{43}$$

For the shock tunnel experiments it is again necessary to know the turbulence level ahead of the probe boundary layer. This may be related to the longitudinal velocity turbulence level (axial component) actually present in the supersonic boundary layer through the Mach number dependent normal shock amplification factor derived by Ribner (Reference 16). This has a perfect gas limit of 1.8 for hypersonic flow diminishing to a value of 1.6 at the point of closest approach to the wall reported by Wallace. For purposes of the present comparison we chose an average amplification factor of 1.7. Thus for hypersonic boundary layers we might expect that for pure vorticity fluctuations ahead of the probe shock a relationship of the form:

$$A = \left(\frac{3.8\,(1.7)}{0.15}\right)\left|v\right|/V_o \tag{44}$$

would properly relate the Sutera parameter A to the turbulence intensity.

In the absence of detailed measurements of $|v|/V_o$ for a hypersonic nozzle boundary layer, we chose to consider simply the Klebanoff (e.g., Ref. 29*) values of longitudinal turbulence intensity. From Figure 2 of the cited reference we find that a value of $|v|/V_o = 0.15/1.7 = 0.088$ occurs at $y/\delta = 0.021$ (also at $y/\delta = 0.002$ but no heat transfer measurements were recorded in the shock tunnel sublayer). Now from Figure 6 we find for the shock tunnel operating conditions ($M_\infty = 7.9$, $T_o = 1800°R$, $R_e/ft = 2.0 \rightarrow 10.0 \times 10^6$) that $E = 0.06$ and for $A = 3.8$, $q/q_b = 2.25$. This is of the order of the measured values of excess heating at $y/\delta = 0.05$ for a number of shock tunnel runs.

Finally a curve of A vs y/δ obtained from Equation 44 and the Klebanoff profile as well as a curve of q/q_b vs y/δ obtained from the curve of A vs y/δ and Figure 6 appear as Figure 7. Included are the values of q/q_b obtained from the shock tunnel measurements. It should be noted that considerable scatter of experimental data prevents a completely satisfactory comparison. However, one sees that the unexpectedly high heating rates measured (in some cases over 100% increase) and their diminution with increased y/δ are on the whole predictable. It may therefore be concluded that this analysis of stagnation zone heating is capable of predicting the high heating rates encountered when the free stream is turbulent.

2. ARC-HEATED WIND TUNNEL TURBULENCE

An in-house program to characterize the turbulence in a typical air arc-heated hypersonic wind tunnel is currently under way at the Air Force Flight Dynamics Laboratory. The initial phase of the program involves measurement of as many forms of unsteady behavior in the tunnel as possible with existing instrumentation and ultimate auto and cross correlation of the data. The analysis has not been completed; however, certain of the preliminary results illustrate the basic nature of the turbulence problem discussed in Section II.

Basically the experiments involved introducing a Kaman model K1808 acoustic transducer, with nearly flat frequency response from 10 Hz to 20,000 Hz and pressure range from 120 to 200 db sound pressure level (SPL), mounted in either a cylindrical or rectangular flat-faced probe into the test effluent of the AFFDL 4-megawatt electrogasdynamics facility (EGF) (Reference 30). (Also see Figure 1.) In order to prevent blocking by the 1 inch x 6 inch rectangular flat-faced stagnation probe, an 18-inch diameter nozzle was utilized. Measurements of heater voltage, pressure, microphone output, as well as the output from an RCA 6217 photomultiplier looking directly at the gas cap radiation were recorded via an Ampex CP 100 FM tape recorder with a frequency range of 0 to 27 kHz.

Of particular interest are the microphone and photomultiplier outputs. A sample of the tape records is presented in Figure 8 and the corresponding power spectra follow in Figures 9a and 9b. One sees that a rather broad spectrum of turbulence exists at the axisymmetric probe, stagnation point.** It is observed from the scope traces that the microphone and photomultiplier display some degree of cross correlation as would be expected. This follows from the fact that under the conditions of the test the upper frequency limit of the microphone (20 kHz) corresponds to a wavelength in the gas cap region of about 0.2 ft. Thus over the

---

* In Reference 29, Figure 2, the component of turbulence intensity in the flow direction is labeled u'/Uo and in our notation this is $|v|/V_o$.

** Very similar power spectral densities occur for the two-dimensional probe tests.

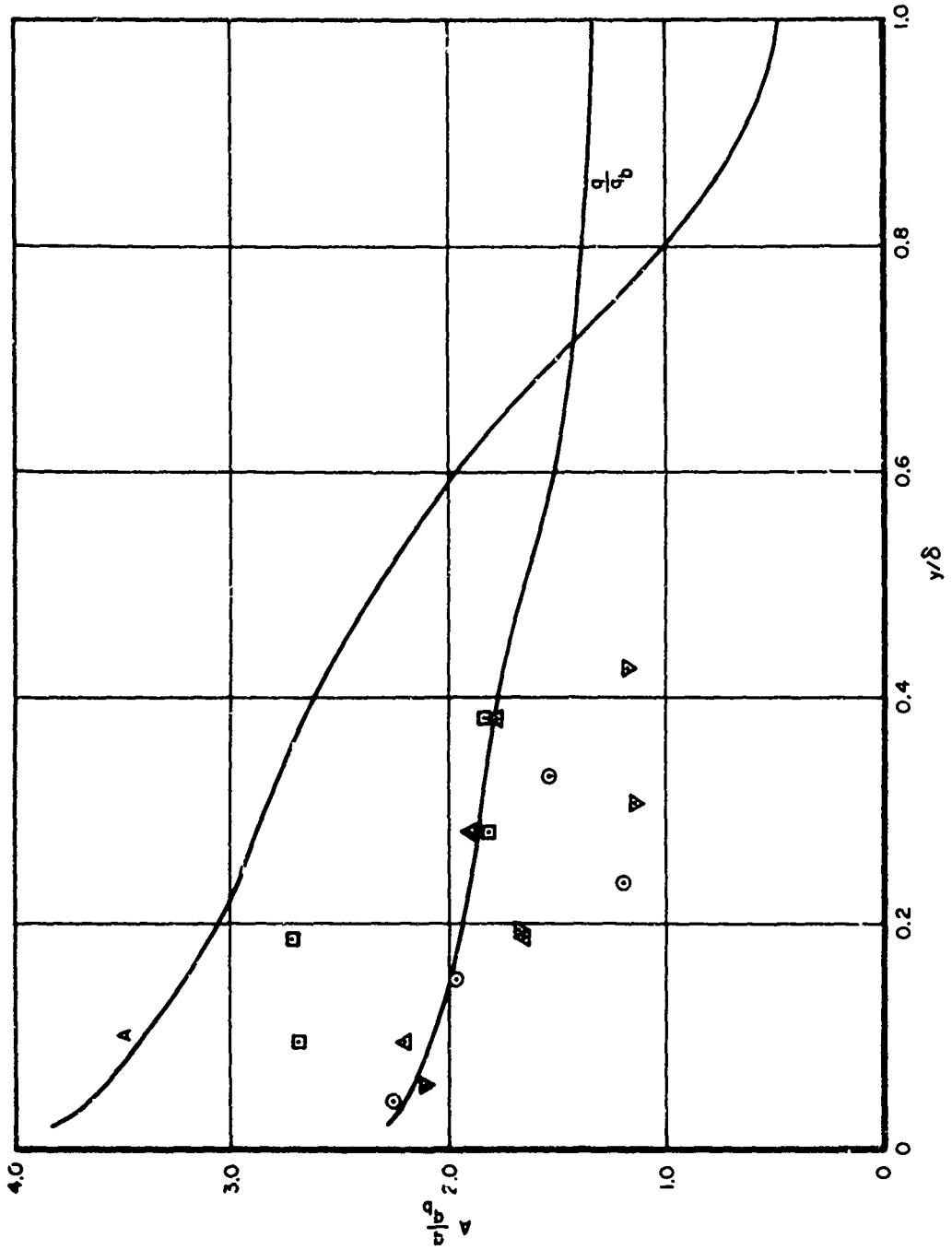

Figure 7. Variation of Stagnation Point Heat Transfer Through a Turbulent Boundary Layer

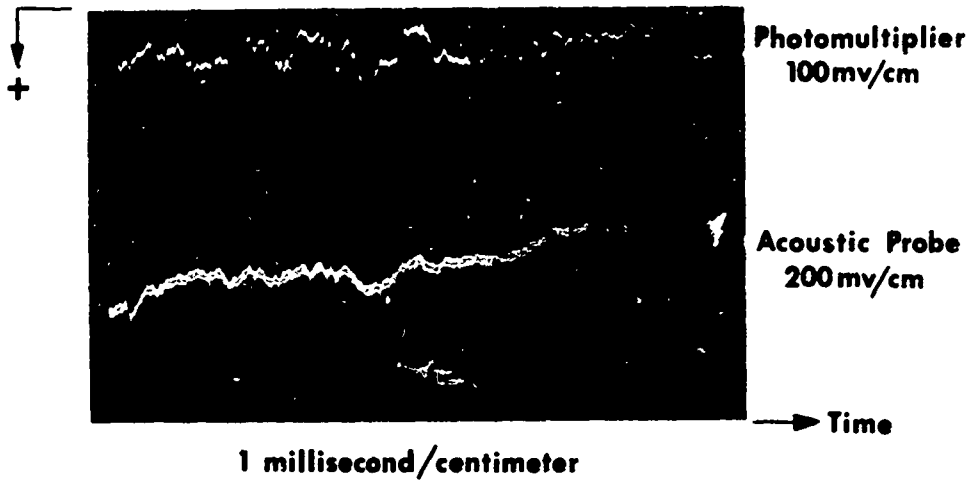

Figure 8. Photomultiplier and Acoustics Probe Oscilloscope Traces (Experimental Configuration Corresponds to Figure 1)

range of frequencies examined, the data corresponds to gross property variations within the entire shock layer. The same considerations based on the foregoing analysis place the cutoff frequency f_o at about 200 kHz. This is based on Sutera's cutoff wavelength λ_o approximately equal to 2.6 times the classical Hiemenz boundary layer thickness (Reference 25) which in turn is set equal to the estimated probe face boundary layer thickness of 0.1 inch. It can thus be stated that velocity disturbances normal to a stagnation line with frequencies below 200 kHz will be amplified upon passing through the boundary layer. The dissipation mechanism, of course, will predominate at higher frequencies.

3. STAGNATION HEATING IN PLASMA JET

Recent measurements of stagnation point heating have been made in a high enthalpy turbulent nitrogen jet exhausting to atmosphere (Reference 31). The jet was produced by a 1.5-megawatt arc heater and was caused to impinge normally on a large instrumented flat plate positioned at several axial stations. Nominal operating conditions reported were: jet exit radius r_e = 0.375 inch, exit Mach number = 0.782, and exit stagnation enthalpy = 4460 BTU/lb giving an exit stagnation temperature of 5000°K. The jet flow has been previously investigated and all important thermodynamic properties are reported in Reference 32.

The measured stagnation point heat transfer rates reported in Reference 31 were compared with the values expected based on the theory of Fay and Riddell. The measured pressure distribution on the plate was employed to establish the required stagnation point velocity gradient. This comparison revealed that the measured stagnation heat flux was between two and three times greater than the laminar theory predicts and it was suggested that this discrepancy was due to the presence of turbulence in the jet.

Previous investigations of the jet via high speed motion pictures revealed relatively little instability. Measurement of sound pressure level, however, revealed a 120-db white noise spectrum over a range from 20 Hz to 10,000 Hz. This result may be compared with the present findings for the hypersonic jet flow case (see ARC-HEATED WIND TUNNEL TURBULENCE in this Section) where again a white noise spectrum is observed.

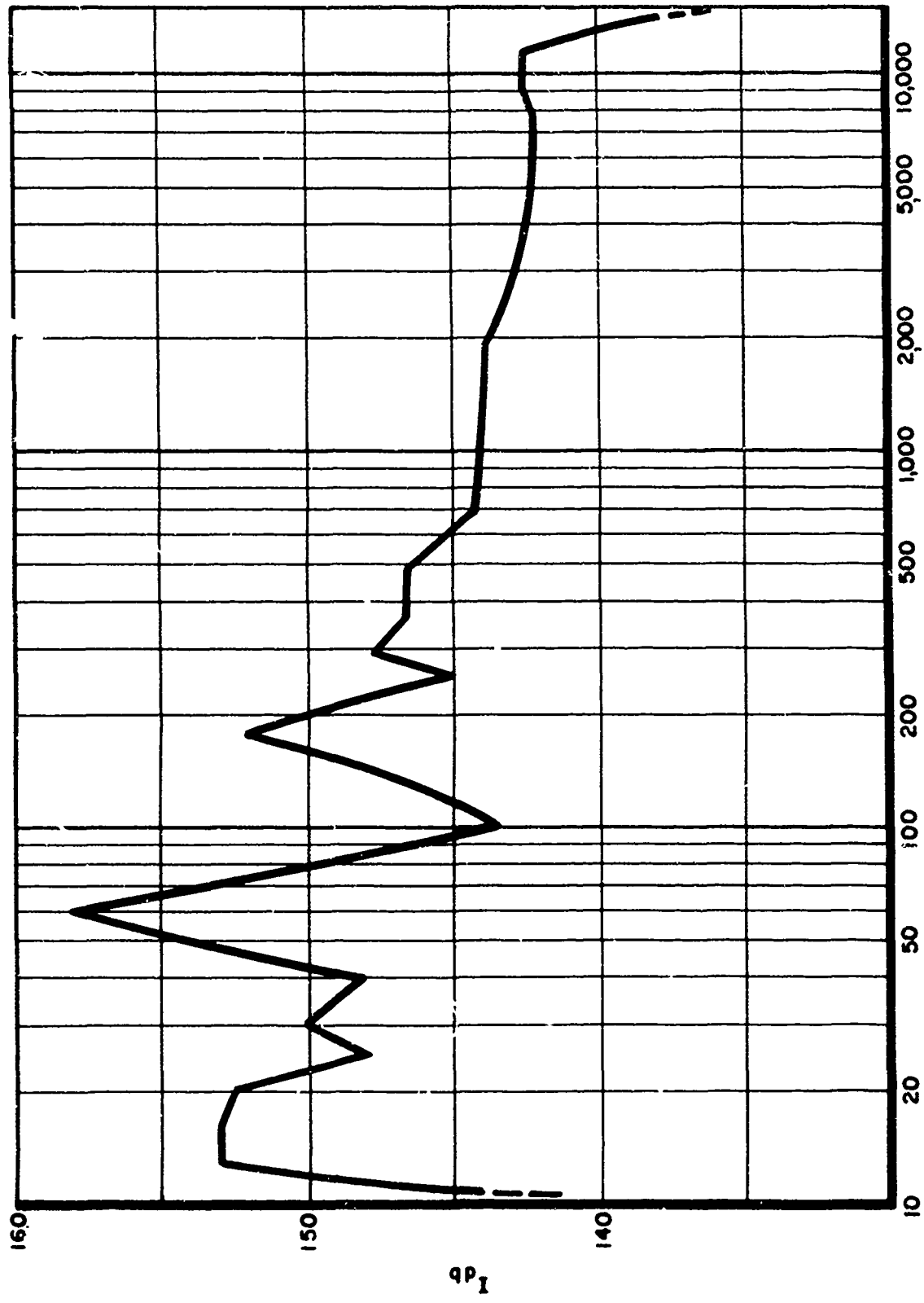

Figure 9a. Power Spectral Density Analysis, Acoustic Probe

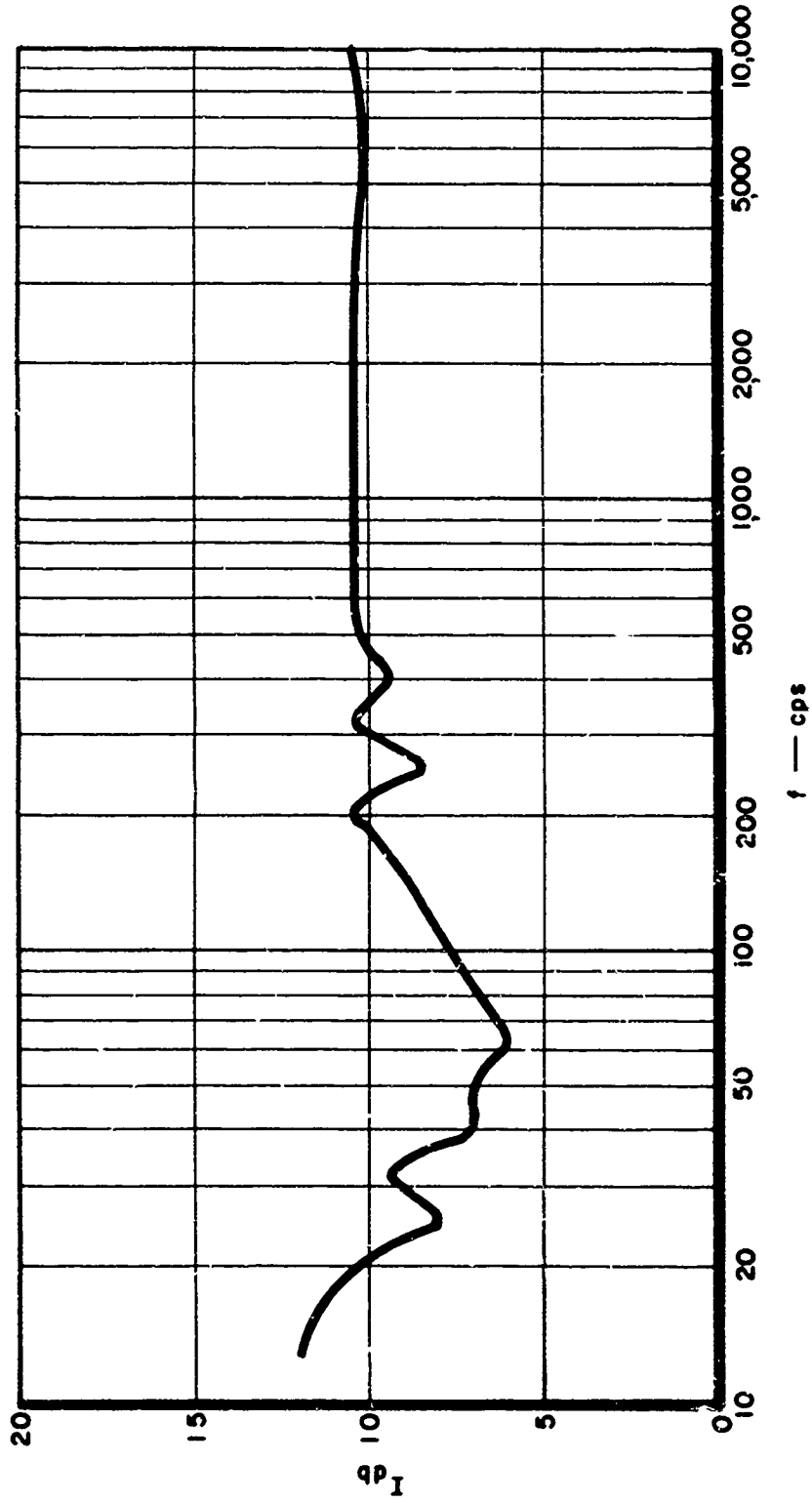

Figure 9b. Power Spectral Density Analysis, Photomultiplier

In an attempt to assess quantitatively the possible effects of free-stream turbulence on the increased stagnation heating, the authors assumed (in the absence of actual turbulence level measurements) that the axial distribution of turbulence intensity was similar to that found by Corrsin and Uberoi (Reference 33). It was assumed that for a particular value of mean velocity, nondimensionalized with respect to the exit velocity, the turbulence level would be that predicted by Corrsin and Uberoi for the same nondimensional mean velocity. Since the axial mean velocity in plasma jet decayed more rapidly than typical cold jet results, the foregoing assumption leads to a somewhat higher turbulence level at a given axial location in the jet.

Both Corrsin and Uberoi's results for the cold jet (u/u_e, T_u vs x/r_e)* and corresponding results for the plasma jet are plotted in Figure 10. Condition (1) in the figure corresponds to the plasma jet results whereas Condition (2) refers to Corrsin and Uberoi's cold jet measurements.

These results may be utilized in conjunction with the present theory to predict the turbulent stagnation heating rates. The procedure is the same as that outlined in this Section under SHOCK TUNNEL TURBULENT NOZZLE BOUNDARY LAYER. Equation 44 relates the parameter A to the measured turbulence level. The Eckert number was again obtained from Equation 42 and was found to vary from 0.12 at the exit to 0.03 at the last data station. Values of q/q_b were calculated, employing Figure 6, corresponding to the turbulence levels given by Conditions (1) and (2). This produced two heating curves which are plotted along with the experimental results in Figure 10. It appears that the experimental results are well bracketed by the theory up to about 25 nozzle exit radii downstream. Beyond this point it might well be expected that errors in heat transfer measurement and plate pressure distribution would accumulate rapidly.

* T_u is the turbulence intensity, u_e and r_e are the nozzle exit velocity and radius, respectively.

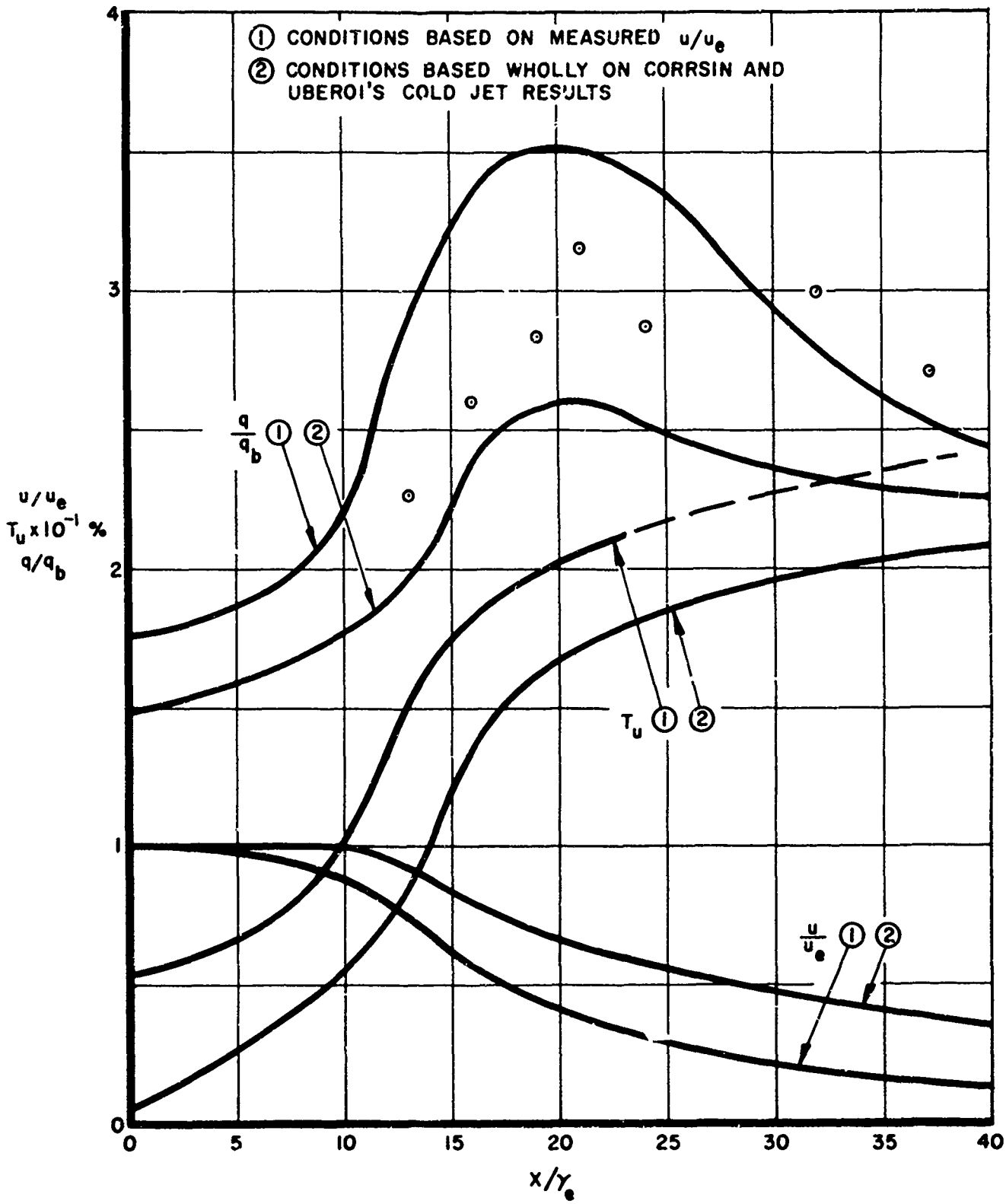

Figure 10. Stagnation Point Heat Transfer Rate Along the Centerline of a Nitrogen Plasma Jet

SECTION V

CONCLUDING REMARKS

The analytical approach discussed in this report appears to provide a means of assessing quantitatively the effects of velocity disturbances ahead of the stagnation point boundary layer on heat transfer. There are several other boundary layer-disturbance interaction problems that must be explored along with a broad class of shock-turbulence interaction problems in order to fully understand the role of free-stream disturbances on hypersonic stagnation zone heat transfer. As a consequence of the favorable agreement between the present analysis and the shock tunnel boundary layer experiments, a number of tentative conclusions can be drawn:

1. The turbulent intensity profile in the hypersonic boundary layer investigated may be approximated by a Klebanoff distribution. The maximum turbulence intensity in the boundary layer would then be of the order of 10%.

2. Amplification at longitudinal turbulence intensities via a normal shock interaction process may be given in the high Mach number limit by Ribner's shock-shear wave interaction analysis.

3. A stagnation point heat transfer probe with dimensions sufficiently small with respect to the smallest energy bearing eddys might be employed successfully to measure free-stream or boundary layer turbulence levels.

The arc-heated wind tunnel results are mostly qualitative but reveal most conclusively that the effluent contains turbulent energy as evidenced by the white noise spectrum. No quantitative estimates of turbulence intensity can be offered at this time and must remain the purpose of further exploration both in the core and shroud flow regions. An order of magnitude analysis involving typical eddy sizes suggests that velocity disturbances normal to a stagnation line with frequencies up to 200 kHz will be amplified upon passing through the boundary layer. The dissipation mechanism will predominate at higher frequencies.

A possibility exists to create stagnation heating rates of the order of twice the laminar value in an arc-heated wind tunnel simulation of high heat transfer-high shear. Such a condition corresponds to condition "C" in Figure 6 where the Eckert number is about the same as for the reported shock tunnel experiments. This might be accomplished by rendering the effluent turbulent in some manner making sure that the longitudinal velocity turbulence level is of the order of 10%.

The plasma jet experiments have served to further corroborate the analytical results. Here again, the actual turbulence level was not measured, but a reasonable assumption is that it corresponds to measured cold jet results.

APPENDIX

LISTING OF SPECTRAL INTERACTION FUNCTIONS

In the following expressions i is a dummy index and quantities with subscripts n-i or i-n are to be replaced with zero whenever their subscripts are negative or zero.

Corresponding to Equation 12 we list the $I_{(\alpha, n)}$:

$$I_{(1,n)} = \sum_{i=1}^{\infty} v_i \left(\theta'_{n+i} + \theta'_{i-n} + \theta'_{n-i}\right)$$

$$I_{(2,n)} = \sum_{i=1}^{\infty} \frac{w_i}{k_i} \left(\theta_{i-n}\, k_{i-n} + \theta_{i+n}\, k_{i+n} - \theta_{n-i}\, k_{n-i}\right)$$

$$I_{(3,n)} = \sum_{i=1}^{\infty} 2u_i \left(u_{i+n} + u_{i-n} + u_{n-i}\right)$$

$$I_{(4,n)} = \sum_{i=1}^{\infty} 2v'_i \left(v'_{i+n} + v'_{n-i} + v'_{i-n}\right)$$

$$I_{(5,n)} = \sum_{i=1}^{\infty} 2w_i \left(w_{i+n} + w_{i-n} + w_{n-i}\right)$$

$$I_{(6,n)} = \sum_{i=1}^{\infty} 2v_i\, k_i \left(\frac{w'_{i-n}}{k_{i-n}} + \frac{w'_{n+i}}{k_{n+i}} - \frac{w'_{n-i}}{k_{n-i}}\right)$$

$$I_{(7,n)} = \sum_{i=1}^{\infty} v_i\, k_i \left(v_{i-n}\, k_{i-n} + v_{i+n}\, k_{i+} - v_{n-i}\, k_{n-i}\right)$$

$$I_{(8,n)} = \sum_{i=1}^{\infty} \frac{w'_i}{k_i} \left(\frac{w'_{i-n}}{k_{i-n}} + \frac{w'_{i+n}}{k_{i+n}} - \frac{w'_{n-i}}{k_{n-i}}\right)$$

Corresponding to Equation 35 we obtain the following $I_{(\alpha,1)}$:

$$I_{(1,1)} = I_{(2,1)} = 0$$

$$I_{3(1)} = 2u_{1(2)}u_{2(2)}$$

$$I_{4(1)} = 2v'_{1(2)}\, v'_{2(2)}$$

$$I_{5(1)} = 2w_{1(2)}\, w_{2(2)}$$

$$I_{6(1)} = w'_{1(2)} v_{2(2)} + w'_{1(2)} v_{2(2)} + w'_{2(2)} v_{1(2)} - \frac{1}{2} w'_{2(2)} v_{1(2)}$$

$$I_{(7,1)} = k_1^2 (v_{1(2)} v_{2(2)} + v_{1(2)} v_{2(2)} + 4 v_{2(2)} v_{1(2)} - 2 v_{2(2)} v_{1(2)})$$

$$I_{(8,1)} = \frac{1}{k_1^2} \left(\frac{w'_{1(2)} w'_{2(1)}}{2} + \frac{w'_{1(2)} w'_{2(2)}}{2} \right)$$

The spectral interaction functions $I_{(\alpha, 2)}$ appearing in Equation 36 are:

$$I_{(1,2)} = v_{1(2)} \theta'_{1(1)}$$

$$I_{(2,2)} = 0$$

$$I_{(3,2)} = u^2_{1(2)}$$

$$I_{(4,2)} = v'^2_{1(2)}$$

$$I_{(5,2)} = w^2_{1(2)}$$

$$I_{(6,2)} = 0$$

$$I_{(7,2)} = k_2^2 v^2_{1(2)}$$

$$I_{(8,2)} = \frac{-1}{k_2^2} w'^2_{1(2)}$$

Finally the $I_{(1,1)}$, $I_{(2,1)}$ corresponding to Equation 38 and the $I_{(1,2)}$, $I_{(2,2)}$ corresponding to Equation 39 are listed.

$$I_{(1,1)} = v_{2(2)} \theta'_{1(1)} + v_{1(2)} \theta'_{2(1)}$$

$$I_{(2,1)} = \frac{3}{2} w_{2(2)} \theta_{1(1)}$$

$$I_{(1,2)} = v_{1(2)} \theta'_{1(2)}$$

$$I_{(2,2)} = w_{1(2)} \theta_{1(2)}$$

REFERENCES

1. S. P. Sutera, "Vorticity Amplification in Stagnation-Point Flow and Its Effect on Heat Transfer," J. Fluid Mech. 21, Part 3, pp. 513-534, 1965.

2. L. S. G. Kovasznay, "Plasma Turbulence," Space Technology Laboratories, Inc., STL/TR-60-0000-AE038, 1960.

3. L. S. G. Kovasznay, "Turbulence in Supersonic Flow," J. Aeronaut Sci. 20, pp. 657-674 and p. 682, 1953.

4. B. T. Chu and L. S. G. Kovasznay, "Non-linear Interactions in a Viscous, Heat Conducting, Compressible Gas," J. Fluid Mech. 3, pp. 494-514, 1958.

5. M. V. Morkovin, "On Supersonic Wind Tunnels with Low Free-Stream Disturbances," J. Appl. Mech. 26, pp. 319-324, 1959.

6. J. Kestin and P. F. Maeder, "Influence of Turbulence on the Transfer of Heat from Cylinders," NACA TN 4018, 1957.

7. J. Kestin, P. F. Maeder, and H. H. Sogin, "The Influence of Turbulence on the Transfer of Heat to Cylinders near the Stagnation-Point," Z. Angew. Math. Phys. 12, pp. 115-132, 1961.

8. R. A. Seban, "The Influence of Free-Stream Turbulence on the Local Heat Transfer from Cylinders," Trans. ASME, Part C, (J. Heat Transfer) 82, pp. 101-107, 1960.

9. W. H. Short, R. A. S. Brown, and B. H. Sage, "Thermal Transfer in Turbulent Gas Streams, Effect of Turbulence on Local Transport from Spheres." J. Appl. Mech 27, pp. 393-402, 1960.

10. W. H. Geidt, "Effect of Turbulence Level of Incident Air Stream on Local Heat Transfer and Skin Friction on a Cylinder," J. Aeronaut Sci. 18, pp. 725-730, 1951.

11. R. D. Brown, "A Comparison of The Theoretical and Experimental Stagnation-Point Heat Transfer in an Arc-Heated Subsonic Stream," NASA TN-D-1927.

12. Dewey C. Forbes, Jr., "Hot-Wire Measurements in Low Reynolds Number Hypersonic Flows, Galcit Memo 63, 1961.

13. M. V. Morkovin, "Aeromechanical Effects in Ablation," J. American Rocket Soc. 30, pp. 429-430, 1960.

14. J. Laufer, "Aerodynamic Noise in Supersonic Wind Tunnels," Jet Propulsion Laboratory, Progress Report 20-378, ORDCIT Contract DA-04-495ORD 18, 1959.

15. M. J. Lighthill, "On the Energy Scattered from the Interaction of Turbulence with Sound or Shock Waves," Proceedings of Cambridge Philosophical Society 49, pp. 531-551, 1953.

16. H. S. Ribner, "Convection of a Pattern of Vorticity Through a Shock Wave," NACA TR 1164, 1954.

REFERENCES (CONT)

17. C. I. Chang, "Interaction of a Plane Shock and Oblique Plane Disturbances, with Special Reference to Entropy Waves," J. Aeronaut Sci. 24, pp. 675-682, 1957.

18. T. M. Weeks and D. S. Dosanjh, "Sound Generation by Shock-Vortex Interaction," AIAA J. 5, pp. 660-669, 1967.

19. D. S. Dosanjh, "Interaction of Concentrated Vorticity with an Advancing Shock and Expansion Wave," Syracuse University Research Institute, Report ME 931-1256-6603-F, 1966.

20. C. W. Haldeman, private communication.

21. M. J. Fisher and F. R. Krause, "Local Measurements in Turbulent Flows Through Cross Correlation of Optical Signals," NASA-MSFC-1268, 1967.

22. G. Trottier, A. M. Ahmed, and D. Ellington, "Cooled Film Anemometer Measurements in the Hypersonic Wake," Canadian Armament Research and Development Establishment, CARDE TN 1720/66.

23. L. M. Fingerson and P. L. Blackshear, "Characteristics of the Heat Flux Meter for Use in High Temperature Atmospheres," University of Minnesota, TR 61-1, 1961.

24. E. P. Muntz, Gas Density Fluctuations in the Hypersonic Turbulent Wake of a Sharp, Slender Cone, General Electric No. 67SD416, BSD TR 67-28, DDC AD 809082, 1967.

25. S. P. Sutera, P. F. Maeder, and J. Kestin, "On the Sensitivity of Heat Transfer in the Stagnation-Point Boundary Layer to Free-Stream Vorticity," J. Fluid Mech. 16, pp. 497-520, 1963.

26. H. Schlichting, Boundary Layer Theory, Pergamon Press, p. 70.

27. A. M. Kuethe and W. W. Wilmarth, "Stagnation-Point Fluctuations on a Body of Revolution," Physics of Fluids 2, pp. 714-716, 1959.

28. J. E. Wallace, "Shock Tunnel Investigations of Turbulent Flow at High Mach Numbers," Cornell Aeronautical Laboratories, Quarterly Progress Report 3, Contract NSR 33-009-029.

29. M. V. Lowson, "Pressure Fluctuations in Turbulent Boundary Layers," NASA TN D3156, 1965.

30. D. Zonars, "Nonequilibrium Regime of Airflows in Contoured Nozzles Theory and Experiments," AIAA J. 5, pp. 57-63, 1967.

31. E. H. Comfort et al, "Heat Transfer Resulting From the Normal Impingement of a Turbulent High Temperature Jet on An Infinitely Large Flat Plate," Reprint of Proceedings of the 1966 Heat Transfer and Fluid Mechanics Institute.

32. T. J. O'Conner et al, "Turbulent Mixing of an Axisymmetric Jet of Partially Dissociated Nitrogen with Ambient Air," AIAA J. 4, pp. 2025-2032, 1966.

33. S. Corrsin and M. S. Uberoi, "Further Experiments on the Flow and Heat Transfer in a Heated Turbulent Air Jet," NACA Report 998, 1950.

UNCLASSIFIED

Security Classification

DOCUMENT CONTROL DATA - R&D

(Security classification of title body of abstract and indexing annotation must be entered when the overall report is classified)

1 ORIGINATING ACTIVITY *(Corporate author)*

Air Force Flight Dynamics Laboratory
Wright-Patterson Air Force Base, Ohio

2a REPORT SECURITY CLASSIFICATION

UNCLASSIFIED

2b GROUP

N/A

3 REPORT TITLE

INFLUENCE OF FREE-STREAM TURBULENCE ON HYPERSONIC STAGNATION ZONE HEATING

4 DESCRIPTIVE NOTES *(Type of report and inclusive dates)*

January 1966 - June 1967

5 AUTHOR(S) *(Last name, first name, initial)*

Weeks, Thomas M, 1/Lt USAF

6 REPORT DATE	7a TOTAL NO. OF PAGES	7b NO. OF REFS
May 1968	42	33

8a CONTRACT OR GRANT NO.	9a ORIGINATOR'S REPORT NUMBER(S)
b PROJECT NO 1426	AFFDL-TR-67-195
c. Task 142604	9b OTHER REPORT NO(S) *(Any other numbers that may be assigned this report)*
d	

10 AVAILABILITY/LIMITATION NOTICES

This document has been approved for public release and sale; its distribution is unlimited.

11. SUPPLEMENTARY NOTES	12. SPONSORING MILITARY ACTIVITY
None	Air Force Flight Dynamics Laboratory Wright-Patterson Air Force Base, Ohio

13 ABSTRACT

The much ignored problem of turbulence in hypersonic ground test facilities is discussed with particular emphasis on arc-heated facilities. Sources of free-stream turbulence and their effects on model aerodynamics are identified. An analytical treatment of stagnation zone heating accounting for free-stream vorticity amplification and viscous dissipation is presented. Results are discussed in relation to three experiments: one involving time resolved measurements in an arc-heated wind tunnel, another involves stagnation point heat transfer measurements in the turbulent boundary layer of a hypersonic shock tunnel, and the third deals with similar measurements in a turbulent subsonic nitrogen plasma jet. In both of the latter experiments, stagnation point heating rates exceeding two to three times the calculated laminar expectation are reported. These results are corroborated by the present analysis.

DD FORM 1 JAN 64 1473

UNCLASSIFIED

Security Classification

14 KEY WORDS	LINK A		LINK B		LINK C	
	ROLE	WT	ROLE	WT	ROLE	WT
Ground/Flight Correlation, Shock Tunnel, Arc-Heated Wind Tunnel, Heat Transfer, Stagnation Zone, Hypersonic Turbulence, Fluid Mechanics, Vorticity Amplification, Viscous Dissipation, Acoustic Probe, Wind Tunnel Dynamics						

INSTRUCTIONS

1. ORIGINATING ACTIVITY: Enter the name and address of the contractor, subcontractor, grantee, Department of Defense activity or other organization *(corporate author)* issuing the report.

2a. REPORT SECURITY CLASSIFICATION: Enter the overall security classification of the report. Indicate whether "Restricted Data" is included. Marking is to be in accordance with appropriate security regulations.

2b. GROUP: Automatic downgrading is specified in DoD Directive 5200.10 and Armed Forces Industrial Manual. Enter the group number. Also, when applicable, show that optional markings have been used for Group 3 and Group 4 as authorized.

3. REPORT TITLE: Enter the complete report title in all capital letters. Titles in all cases should be unclassified. If a meaningful title cannot be selected without classification, show title classification in all capitals in parenthesis immediately following the title.

4. DESCRIPTIVE NOTES: If appropriate, enter the type of report, e.g., interim, progress, summary, annual, or final. Give the inclusive dates when a specific reporting period is covered.

5. AUTHOR(S): Enter the name(s) of author(s) as shown on or in the report. Enter last name, first name, middle initial. If military, show rank and branch of service. The name of the principal author is an absolute minimum requirement.

6. REPORT DATE: Enter the date of the report as day, month, year, or month, year. If more than one date appears on the report, use date of publication.

7a. TOTAL NUMBER OF PAGES: The total page count should follow normal pagination procedures, i.e., enter the number of pages containing information.

7b. NUMBER OF REFERENCES: Enter the total number of references cited in the report.

8a. CONTRACT OR GRANT NUMBER: If appropriate, enter the applicable number of the contract or grant under which the report was written.

8b, 8c, & 8d. PROJECT NUMBER: Enter the appropriate military department identification, such as project number, subproject number, system numbers, task number, etc.

9a. ORIGINATOR'S REPORT NUMBER(S): Enter the official report number by which the document will be identified and controlled by the originating activity. This number must be unique to this report.

9b. OTHER REPORT NUMBER(S): If the report has been assigned any other report numbers *(either by the originator or by the sponsor)*, also enter this number(s).

10. AVAILABILITY/LIMITATION NOTICES: Enter any limitations on further dissemination of the report, other than those imposed by security classification, using standard statements such as:

(1) "Qualified requesters may obtain copies of this report from DDC."

(2) "Foreign announcement and dissemination of this report by DDC is not authorized."

(3) "U. S. Government agencies may obtain copies of this report directly from DDC. Other qualified DDC users shall request through

_____."

(4) "U. S. military agencies may obtain copies of this report directly from DDC. Other qualified users shall request through

_____."

(5) "All distribution of this report is controlled. Qualified DDC users shall request through

_____."

If the report has been furnished to the Office of Technical Services, Department of Commerce, for sale to the public, indicate this fact and enter the price, if known.

11. SUPPLEMENTARY NOTES: Use for additional explanatory notes.

12. SPONSORING MILITARY ACTIVITY: Enter the name of the departmental project office or laboratory sponsoring *(paying for)* the research and development. Include address.

13. ABSTRACT: Enter an abstract giving a brief and factual summary of the document indicative of the report, even though it may also appear elsewhere in the body of the technical report. If additional space is required, a continuation sheet shall be attached.

It is highly desirable that the abstract of classified reports be unclassified. Each paragraph of the abstract shall end with an indication of the military security classification of the information in the paragraph, represented as *(TS)*, *(S)*, *(C)*, or *(U)*.

There is no limitation on the length of the abstract. However, the suggested length is from 150 to 225 words.

14. KEY WORDS: Key words are technically meaningful terms or short phrases that characterize a report and may be used as index entries for cataloging the report. Key words must be selected so that no security classification is required. Identifiers, such as equipment model designation, trade name, military project code name, geographic location, may be used as key words but will be followed by an indication of technical context. The assignment of links, rules, and weights is optional.